Infrasound from the 2009 and 2017 DPRK rocket launches

Evers, L. G.; Assink, J. D.; Smets, P. S.M.

DOI
10.1093/gji/ggy092

Publication date
2018

Document Version
Final published version

Published in
Geophysical Journal International

Geophysical Journal International

Geophys. J. Int. (2018) **213,** 1785–1791
Advance Access publication 2018 March 9
GJI Seismology

doi: 10.1093/gji/ggy092

Infrasound from the 2009 and 2017 DPRK rocket launches

L.G. Evers,[1,2] J.D. Assink[1] and P.S.M. Smets[1,2]

[1] *Department of Seismology and Acoustics, Royal Netherlands Meteorological Institute, Utrechtseweg* 297, 3731 *GA De Bilt, The Netherlands.*
E-mail: evers@knmi.nl
[2] *Department of Geoscience and Engineering, Faculty of Civil Engineering and Geosciences, Delft University of Technology, Stevinweg* 1, 2628 *CN Delft, The Netherlands*

Accepted 2018 March 8. Received 2018 February 16; in original form 2017 November 21

SUMMARY

Supersonic rockets generate low-frequency acoustic waves, that is, infrasound, during the launch and re-entry. Infrasound is routinely observed at infrasound arrays from the International Monitoring System, in place for the verification of the Comprehensive Nuclear-Test-Ban Treaty. Association and source identification are key elements of the verification system. The moving nature of a rocket is a defining criterion in order to distinguish it from an isolated explosion. Here, it is shown how infrasound recordings can be associated, which leads to identification of the rocket. Propagation modelling is included to further constrain the source identification. Four rocket launches by the Democratic People's Republic of Korea in 2009 and 2017 are analysed in which multiple arrays detected the infrasound. Source identification in this region is important for verification purposes. It is concluded that with a passive monitoring technique such as infrasound, characteristics can be remotely obtained on sources of interest, that is, infrasonic intelligence, over 4500+ km.

Key words: Acoustic-gravity waves; Time-series analysis; Earthquake monitoring and test-ban treaty verification; Wave propagation.

1 INTRODUCTION

Infrasound from rockets was first studied by infrasound researchers of the Lamont-Doherty Geological Observatory of Columbia University, USA, in the late sixties of the last century. A first observation of infrasound from a Saturn V rocket was reported in Donn *et al.* (1968) by the researchers. Balachandran *et al.* (1971) further showed how stratospheric winds positively influence the detectability of infrasound from rockets in the downwind direction. Stratospheric winds also appeared to control the signal amplitude and duration (Balachandran & Donn 1971).

A remarkable observation was described by Cotten & Donn (1971), where infrasound was observed from a rocket flying over an infrasound array at 188 km altitude. Cotten *et al.* (1971) explained this rare observation by the exhaust plume generating shock cones, which couple to sound waves in the denser lower atmosphere.

In 1996, the Comprehensive Nuclear-Test-Ban Treaty (CTBT) opened for signature. Within its International Monitoring System (IMS), infrasound is applied as a verification technique for atmospheric nuclear test explosions (Dahlman *et al.* 2009). Out of the 60 planned infrasound arrays, currently 49 arrays are certified and sending data in real-time to the International Data Center in Vienna (status in September 2017). Observations of infrasound from rockets on the IMS infrasound arrays are routinely made as shown, for example, by Campus & Christie (2009) and Blom *et al.* (2016), as expected from the earlier studies.

Identifying the source of transient infrasound signals is the ultimate goal for infrasound as a verification technique. This process starts with detection followed by association. Preferably, multiple arrays are used to enable localization through cross bearing (Le Pichon *et al.* 2009). Distinguishing explosions from other sources, such as rockets, requires the extraction of specific signal features that allow the identification of, for example, a moving source or an extended source time function.

The Democratic People's Republic of Korea (DPRK) has launched several rockets over the last decades, as follows from news reports and press releases by the DPRK. Multiple arrays have detected infrasound from the 2009 April 5, 2017 May 13, 2017 August 28 and 2017 September 14 rocket tests of which some possibly had their flight path over Japan. These launches were chosen to show the infrasonic signatures of the thrust phases during the launch and those associated with the re-entry. The IMS arrays which detected the rocket associated infrasound are located in Japan (I30JP), Mongolia (I34MN), the Russian Federation (I44RU, I45RU, I46RU) and the US (I53US). Fig. 1(a) shows the locations of the arrays, which surround the DPRK.

In this study, it is shown how the moving nature of rockets allows for distinguishing it from a static explosion. Detections from rockets will be analysed at ranges over 4500 km, which is one of the largest distances reported up to now. The propagation of such infrasound is challenging to understand and model under the variable stratospheric conditions near the equinoxes. Furthermore, the

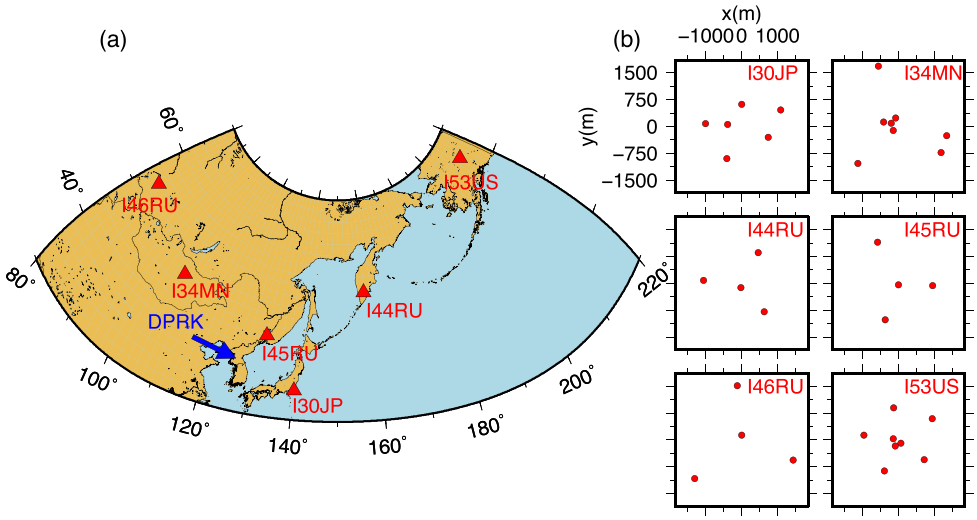

Figure 1. (a) Map with the locations of the IMS infrasound arrays, which surround the Democratic People's Republic of Korea (DPRK). The blue arrow points towards the DPRK. (b) The locations of the microbarometers of each IMS array. The array configurations vary from 4 to 8 microbarometers, with apertures up to 2.5 km. Shown are I30JP in Japan, I34MN in Mongolia, I44RU, I45RU, I46RU in the Russian Federation and I53US in the US.

use of infrasound as a passive monitoring technique is addressed in remotely obtaining information on sources of interest.

2 DATA ACQUISITION AND PROCESSING

Infrasound is measured with arrays of microbarometers (Christie & Campus 2009). Arrays are used to characterize the transient signals in terms of backazimuth and apparent velocity. For this, the time differences or phase delays are used to determine the angle of arrival of the signals with respect to North, that is, the backazimuth. Similarly, the horizontal propagation velocity of the energy over the array is retrieved, called the apparent velocity. Its value can range from infinity, for vertically incident signals, to the local sound speed for horizontally propagating signals. The specific array configurations for extracting these signals characteristics are given in Fig. 1(b). The number of microbarometers per array varies from 4 to 8, while the aperture has values up to 2.5 km.

Beamforming in the time domain combined with a correlation (Melton & Bailey 1957; Cansi 1995) or coherency measure in the frequency domain (Smart & Flinn 1971) is applied for signal detection and characterization. Here, the Fisher ratio analysis is applied, as used for example in Assink *et al.* (2016), which is a measure of the signal-to-noise ratio (SNR).

2.1 The 2009 April 5 rocket launch

It was reported that a rocket was launched from Tonghae Satellite Launching Ground (Musudan-ri) in the northeast of the DPRK on 2009 April 5 (http://www.38north.org/2016/02/melleman021016, last accessed 2017 September 18), around 02h30 UTC.

Fig. 2 shows the array processing results for I45RU, I30JP, I44RU and I53US. The time windows are chosen such that infrasound from the region around the DPRK is included. These windows are based on the information about the launch and flight, taking into account a propagation time based on (along ground) velocities between 0.2 and 0.36 km s^{-1}. It should be noted that there is a shift towards lower frequencies and a decrease in best beam amplitude as a function of distance. Furthermore, the waveforms become more emergent with increasing distance, loosing their impulsive shapes, which are still present at nearby array I45RU. Events are identified on the basis of an increase in SNR, with respect to the background noise. In addition, the retrieved backazimuth values and apparent velocities appear as continuous lines for events, rather than being randomly distributed, which is the case for noise. Apparent velocity around the sound speed (330-340 m s^{-1}) are resolved for events, meaning that a coherent and near horizontal infrasound wave has travelled over the array. Table 1 gives the signal characteristics at maximum SNR, for an array and event-specific frequency pass-band (last column).

Fig. 3(a) shows the retrieved backazimuths on a geographical map. If the backazimuth has a range of values, rather than one distinct value, the beginning and end of the azimuthal variation is plotted (see e.g. I53US). The International Civil Aviation Organization (ICAO) was informed by the DPRK prior to the launch. In a news release from the ICAO on 2009 March 12 (PIO: 02/09) two danger areas were listed, which are also shown in Fig. 3(a), in the Sea of Japan and the Pacific Ocean. The backazimuths point to launch site (I44RU, I45RU and I30JP), to danger area I (I30JP and I44RU) and to danger area II (I53US). The detections at the latter are made at a range over 4500 km, which is one of the largest distance for infrasound from rockets reported up to now.

The above results indicate that the recorded infrasound is associated with the rocket launch, based on the travel time, (cross-bearing of) the backazimuths and the signal characteristics. Further evidence comes from the eastward movement, as retrieved from the backazimuth variations, near the launch site, and at danger zones I and II.

2.2 The 2017 rocket launches

The DPRK launched several rockets in 2017. Here, three launches are investigated because these had multiple array detections and two of these possibly flew over Japan. The presentation of the processing results is similar to Fig. 2 and given as Supporting Information (Figs S1–S3). The signal characteristics are given in Table 1.

A rocket was launched from Kusong, in the northwest of the DPRK, on 2017 May 13 (http://www.38north.org/2017/05/hwasong051917, last accessed 2017 September 29), around 20h27

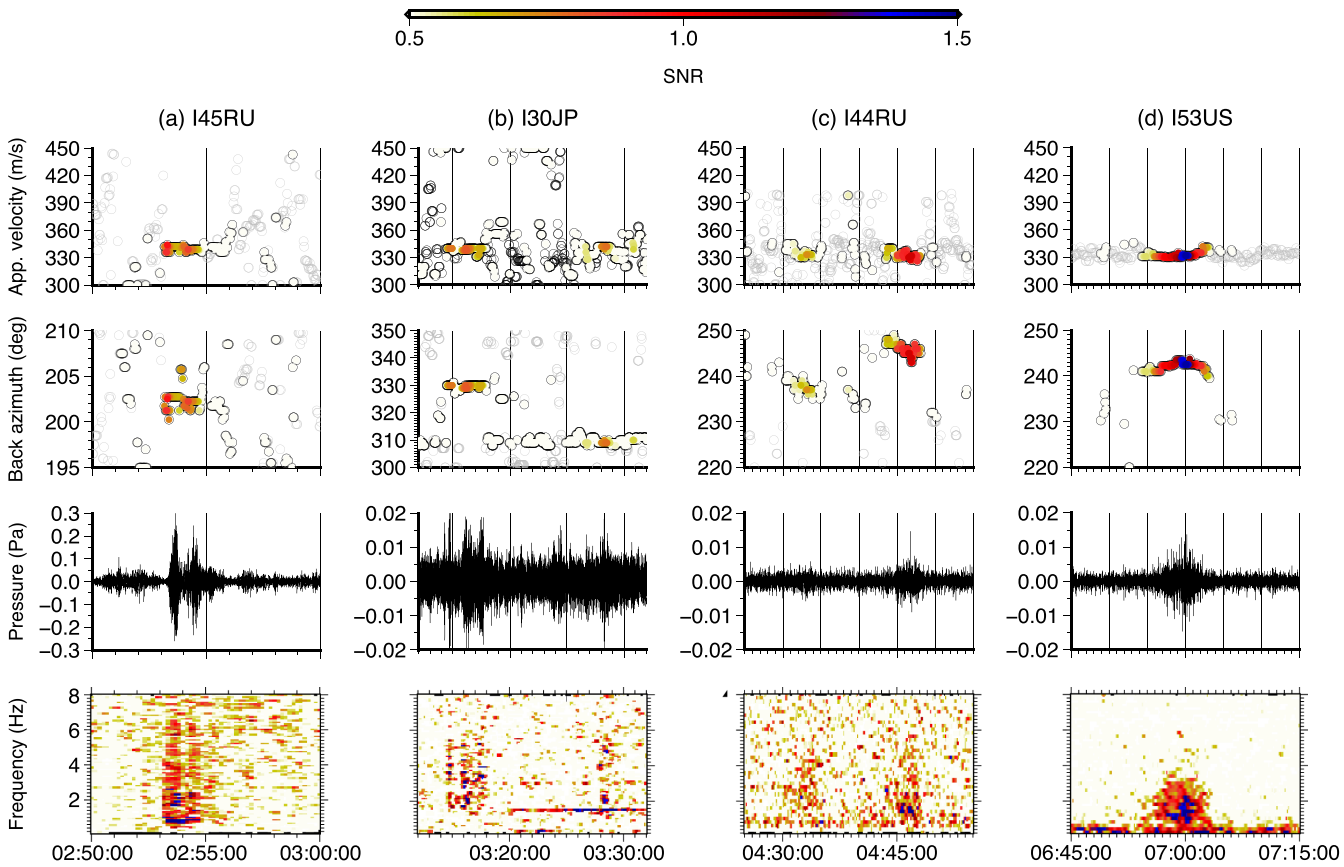

Figure 2. Array processing results for the launch on 2009 April 5. The columns show the results per array, with increasing distance from the source, that is, from left to right (a) I45RU, (b) I30JP, (c) I44RU and (d) I53US. The rows give a parameter, which results from the array processing, as a function of time (UTC) for each array. From bottom to top are given: frequency, amplitude of the best beam, backazimuth and apparent velocity. The parameters are colour coded as a function of the signal-to-noise ratio (SNR). The best beam is calculated for the backazimuth and the apparent velocity at maximum SNR.

Table 1. Signal characteristics at maximum SNR.

Array/ Distance (km)[a]	Time (UTC)	SNR	App. vel. (m s^{-1})	Back azi. (deg)	P2P ampl. (Pa)	Freq. (Hz)	Pass-band (Hz)
2009 April 5	Musudan-ri						
I45RU / 400	02:53:15	1.0	341.8	202.7	0.70	1.0	0.5–7.0
I30JP / 700	03:16:00	0.8	339.0	329.5	0.04	1.5	0.7–3.0
I30JP / 1050	03:28:15	0.8	342.0	309.0	0.04	1.5	
I44RU / 2150	04:33:10	0.7	333.0	236.9	0.01	1.0	0.7–2.0
I44RU / 2500	04:47:00	1.1	330.9	244.0	0.01	0.6	
I53US / 4600	07:00:00	1.5	331.8	242.5	0.03	0.7	0.5–3.0
2017-05-13	Kusong						
I34MN / 1750	22:09:00	1.4	336.0	113.0	0.03	0.8	0.3–3.0
I34MN / 2250	23:08:00	1.8	339.5	97.0	0.04	0.7	
I46RU / 3800	00:38:00	0.6	335.5	92.0	0.01	0.6	0.3–3.0
2017-08-28	Sunan						
I45RU / 700	21:39:45	0.8	356.2	219.2	0.02	0.1	0.1–1.5
I45RU / 750	21:43:30	1.2	381.2	224.0	0.07	0.1	
I44RU / 1200	22:25:00	1.1	336.5	181.7	0.02	1.0	0.3–3.5
2017-09-14	Sunan						
I45RU / 700	22:40:00	1.5	339.8	223.2	0.12	1.0	0.5–4.0
I53US / 3900	01:48:00	1.0	336.5	246.2	0.02	1.0	0.5–2.5

[a]A rough indication of the source–receiver distance.

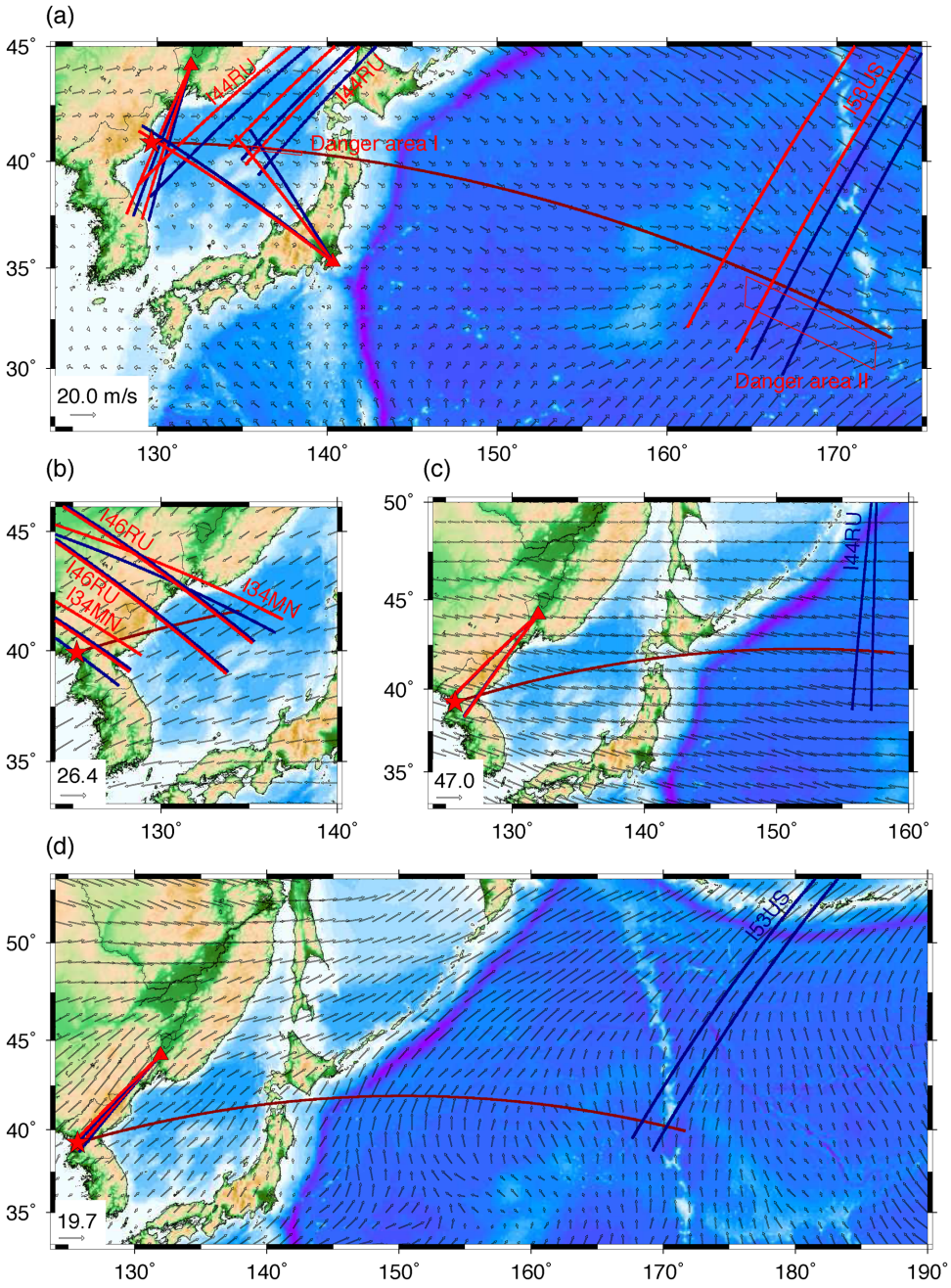

Figure 3. Geographical maps with the launch sites in the DPRK (red stars), observed backazimuths (blue lines) and wind corrected backazimuths (red lines). The dark red line is a rough estimate of the rocket's trajectory, based on news report, and serves as an indication. The black vectors show the wind strength and direction from ECMWF atmospheric conditions at 50 km altitude around the time of the launch. (a) The 2009 April 5 launch from the Tonghae Satellite Launching Ground, the zones enclosed with thin red lines are the pre-announced danger areas, in the Sea of Japan and Pacific Ocean. The backazimuth from I45RU, I30JP, I44RU and I53US are given. (b) The 2017 May 13 launch from Kusong with backazimuths from I34MN and I46RU. (c) Backazimuths from I45RU and I44RU for the 2017 August 28 launch from Pyongyang International Airport (Sunan). (d) A launch was conducted from Pyongyang International Airport on 2017 September 14. Signals were recorded at I45RU and I53US of which the backazimuths are shown.

UTC. Infrasound was detected over long ranges in Mongolia (I34MN) and the centre of the Russian Federation (I46RU). Supporting Information Fig. S1 shows the detections and their characteristics. Clear arrivals are extracted at I34MN. Two distinct packages of energy arrive from the region around the DPRK at the expected time. Further away at I46RU, the signal is less clear as the SNR has lowered due to the longer propagation path. The higher frequencies are also lost, compared to I34MN. However, the travel time and backazimuths are in agreement with the launch, as are those from I34MN (see Fig. 3b).

On 2017 August 28 around 21h UTC, a rocket was launched from Pyongyang International Airport (Sunan). It was reported that this rocket flew over Japan (http://www.38north.org/2017/08/melleman083017/, last accessed 2017 September 27). Clear signals were detected at the expected time of arrival on I45RU and I44RU (see Supporting Information Fig. S2). The signals originate

from directions corresponding to the assumed rocket's trajectory (see Fig. 3c). The resolved backazimuth at I44RU shows a distinct pattern of eastward movement. The detections at I45RU appear to indicate westward movement, due to the reversed sequence of infrasound signals. Earlier detections are from sections of the trajectory closer to the station, such that the earlier generated infrasound is detected later. Therefore, the I45RU signals are also consistent with an eastward rocket trajectory.

The Pyongyang International Airport (Sunan) was also the location for the rocket launch of 2017 September 14 (https://www.38north.org/2017/09/rfrank091817, last accessed 2017 September 27). It was reported that a rocket was launched around 22h UTC, which again flew over Japan. The detections made at I45RU and I53US are shown in Supporting Information Fig. S3. The nearby impulsive signature is captured by I45RU. The high frequencies are damped by the time signals arrive at I53US. The long propagation path also leads to a more emergent signal. Fig. 3(d) shows the observed backazimuths on a geographical map also indicating the eastward movement.

In order to further constrain the signal's nature, propagation modelling is conducted with actual state-of-the-art atmospheric conditions from the European Centre for Medium-Range Weather Forecasts (ECMWF).

3 PROPAGATION MODELLING

Long range infrasound propagation is facilitated by three waveguides in the atmosphere, which refract the upward travelling sound waves back to the earth's surface. Gradients in wind and temperature results in infrasound refraction from the tropopause, stratopause and/or mesopause regions. Stratospheric refractions, from 50 km altitude, dominate in long range, more than 1000 km, sound propagation (Evers *et al.* 2012). At closer stations, tropospheric ducting is also possible, where a significant portion of the energy can leak into the stratosphere depending on the strength of the jetstream.

The Northern Hemisphere stratospheric surf zone, between 20 and 60°N, is characterized by a stable westward circumpolar flow in summer and a variable eastward vortex in winter (McIntyre & Palmer 1984). As such, the atmosphere is an anisotropic medium as detection preferably occurs down wind (Hedlin *et al.* 2010), either east- or westwards. At mid-latitudes in summer, the vortex reaches values up to 50 m s^{-1}, while in winter values over 150 m s^{-1} are possible (Evers *et al.* 2012). In winter, planetary waves from the troposphere couple to the stratosphere and can give rise to Sudden Stratospheric Warmings, which strongly influence long range infrasound propagation (Evers & Siegmund 2009; Smets *et al.* 2016).

The wind strengths and directions are shown as vectors in Fig. 3. All launches took place between the vernal (March 20) and autumnal equinox (September 22). The 2009 April 5 and 2017 September 14 took place close to the equinoxes, respectively 16 d after and 8 d before. Near the wind reversal the wind strength is low and the vortex is not well developed as can be seen in Figs 3(a) and (d).

Cross winds from the jetstream (∼10 km) or circumpolar vortex (∼50 km) will lead to a deviation of the backazimuth (Smets *et al.* 2016). In other words, the retrieved backazimuth does not point to the true source location. In order to correct for this, an in-house developed 3-D ray tracer is used to determine the deviation based on wind and temperature conditions from the ECMWF's analysis. The red lines in Fig. 3 show the wind corrected backazimuths. In the cases considered here, deviations up to 5.3° are found.

The combination of 3-D ray tracing and ECMWF atmospheric conditions does not always explain the observations, as is the case for I44RU on 2017 August 28 and I53US on 2017 September 14. Assink *et al.* (2014) also found that observations from near-continuous volcanic infrasound could not be modelled with a similar approach, for weeks around the equinoxes. Outside equinox periods, Nippress & Green (2017) showed that the IMS is very sensitive to sources in elevated waveguides like the stratosphere, when the waveguide is well-formed. Energy for such elevated sources can also leak from the stratosphere into the troposphere.

Fig. 4 shows the infrasonic propagation for 2009 April 5, which is determined by backward propagation from the receiver to the source, using an effective sound speed. The eigenray trajectories are shown connecting the area above the launch site to the arrays I45RU, I30JP and I44RU. The 3-D ray tracer is used and applied to atmospheric conditions from the ECMWF at 00 UTC. The amplitudes are derived with a 2-D Parabolic Equation (PE) model from Collins (1993), as also applied by, for example, Assink *et al.* (2016). The eigenray search revealed different altitudes from which the infrasonic energy can reach the receivers. I44RU and I45RU detected the energy originating from between 30 and 45 km altitude up in the stratosphere. Energy from a similar altitude range may have coupled into the troposphere to reach I30JP. The tropospheric duct may guide energy generated within the troposphere, around the tropopause, to I30JP.

The complex propagation characteristics show that temporal and spatial variations in detectability of infrasound need to be taken into account for source identification. Infrasound from a source of interest might appear at a recording station, if the atmospheric conditions allow for that.

4 DISCUSSION AND CONCLUSION

The recorded infrasound can be associated to known rocket launches, based on variations in backazimuth, localization through cross-bearing, travel time analysis and waveform characteristics as a function of distance. The association can be further constrained with propagation modelling, using actual atmospheric conditions. Confidence in the interpretation of the signals is gained from the analysis of four cases, showing similar results. The backazimuth variations are also consistently retrieved indicating that this is a source characteristic rather than an uncertainty in the measurement and processing (which is estimated at less than 1°).

The retrieved backazimuths point towards both the launch site and the first part of the supersonic flight, an eastward movement. The rocket is acoustically invisible as it leaves the atmosphere. Upon re-entry, it can be tracked again and an eastward movement is retrieved. Shock waves are typically starting to be generated at an altitude between 80 and 90 km. The latter follows from the study of meteors, which enter the earth's atmosphere at hypersonic speeds (Popova *et al.* 2013). Explosions of the remainders of the rocket will also leave an infrasonic signature.

As shown, the launch and re-entry of stages or the rocket itself can be detected by multiple arrays. This will lead to the association of individual array detections into an event, in an operational environment. The association procedure is preferably an automated algorithm applied to regional (Arrowsmith *et al.* 2008) or global networks like the IMS (Arora *et al.* 2013). The moving nature of the source is important for its identification. Furthermore, the

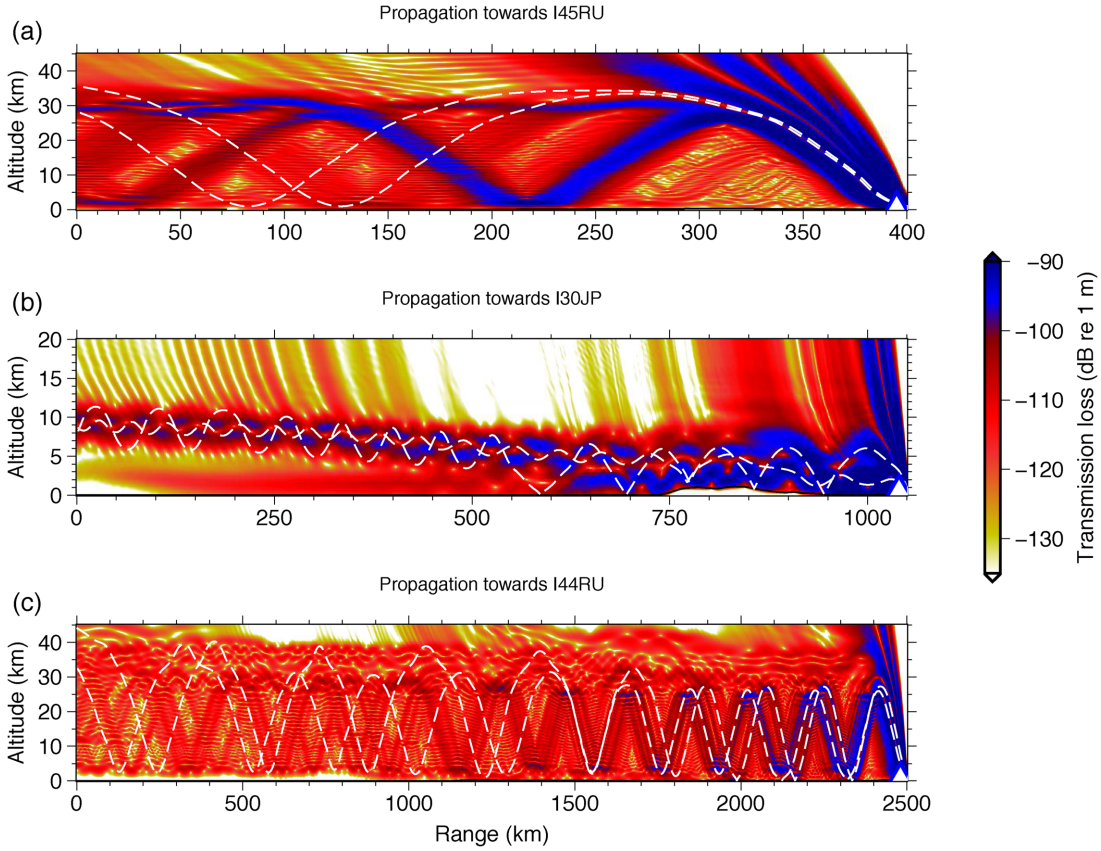

Figure 4. Backward propagation of the infrasonic ray trajectories (white dashed lines) and amplitudes (colours in dB) to the launch site for 2009 April 5. The propagation modelling is shown for (a) I45RU, (b) I30JP and (c) I44RU. The eigenray trajectories are determined with an in-house developed 3-D ray tracer, the amplitudes follow from a 2-D PE model. Atmospheric conditions for wind and temperature are from the analysis of ECMWF at 00 UTC.

same source will show up at different locations, possibly separated by 1000+ km. Capturing these characteristics is currently not undertaken by state-of-the-art association algorithms, but will need to be incorporated in order to classify the signal as being due to a rocket rather than a series of point source like explosion at different locations.

It is concluded that characteristics on sources of interest, like rockets, can be passively and remotely obtained by monitoring atmospheric infrasound, that is, infrasonic intelligence, over ranges of 4500+ km. Future studies will concentrate on retrieving the trajectory by inverting the travel time and backazimuths, and their deviations, for 3-D trajectory segments. Instead of using for example the ECMWF analysis, ensembles will be used to allow for perturbations in the wind and temperature (Smets *et al.* 2015).

Furthermore, a more extensive analysis of all DPRK rocket launches will reveal the detectability of infrasonic signals as a function of the source type and atmospheric conditions.

ACKNOWLEDGEMENTS

The CTBTO and IMS station operators are thanked for the high-quality data and products. IMS infrasound data are available from the CTBTO's virtual Data Exploitation Centre (see https://www.ctbto.org/specials/vdec, last accessed: 2017 August 30). Läslo Evers' contribution is partly funded through a VIDI project from the Netherlands Organisation for Scientific Research (NWO), project number 864.14.005. PS is funded by the ARISE2 project from the European Commission H2020 program (grant number 653980). Figures in this article are made with the Generic Mapping Tools (Wessel & Smith 1991).

REFERENCES

Arora, N.S., Russell, S. & Sudderth, E., 2013. NET-VISA: network processing vertically integrated seismic analysis, *Bull. seism. Soc. Am.,* **103**(2A), 709–729.

Arrowsmith, S.J. *et al.*, 2008. Regional monitoring of infrasound events using multiple arrays: application to Utah and Washington State, *Geophys. J. Int.,* **175**(1), 291–300.

Assink, J.D., Pichon, A.L., Blanc, E., Kallel, M. & Khemiri, L., 2014. Evaluation of wind and temperature profiles from ECMWF analysis on two hemispheres using volcanic infrasound, *J. geophys. Res.,* **119**(14), 8659–8683.

Assink, J.D., Averbuch, G., Smets, P.S.M. & Evers, L.G., 2016. On the infrasound detected from the 2013 and 2016 DPRK's underground nuclear tests, *Geophys. Res. Lett.,* **43**(7), 3526–3533.

Balachandran, N.K. & Donn, W.L., 1971. Characteristics of Infrasonic Signals from Rockets, *Geophys. J. Int.,* **26**(1–4), 135–148.

Balachandran, N.K., Donn, W.L. & Kaschak, G., 1971. On the Propagation of Infrasound from rockets: effects of winds, *J. acoust. Soc. Am.,* **50**(2A), 397–404.

Blom, P., Marcillo, O. & Arrowsmith, S., 2016. Analysis and modeling of infrasound from a four-stage rocket launch, *J. acoust. Soc. Am.,* **139**(6), 3134–3138.

Campus, P. & Christie, D.R., 2009. Worldwide Observations of Infrasonic Waves, in *Infrasound Monitoring for Atmospheric Studies,* chap. 6, pp. 185–234, eds Le Pichon, A., Blanc, E. & Hauchecorne, A., Springer Netherlands.

Cansi, Y., 1995. An automatic seismic event processing for detection and location: the P.M.C.C. method, *Geophys. Res. Lett.,* **22**(9), 1021–1024.

Christie, D.R. & Campus, P., 2009. The IMS infrasound network: design and establishment of infrasound stations, in *Infrasound Monitoring for Atmospheric Studies,* chap. 2, pp. 29–75, eds Le Pichon, A., Blanc, E. & Hauchecorne, A., Springer Netherlands.

Collins, M.D., 1993. A split-step Padé solution for the parabolic equation method, *J. acoust. Soc. Am.,* **93**(4), 1736–1742.

Cotten, D. & Donn, W.L., 1971. Sound from Apollo rockets in space, *Science,* **171**(3971), 565–567.

Cotten, D.E., Donn, W.L. & Oppenheim, A., 1971. On the generation and propagation of shock waves from Apollo rockets at orbital altitudes, *Geophys. J. R. astr. Soc.,* **26**(1–4), 149–159.

Dahlman, O., Mykkeltveit, P. & Haak, H., 2009. Monitoring technologies, in *Nuclear Test Ban,* chap. 2, pp. 1–34, Springer.

Donn, W.L., Posmentier, E., Fehr, U. & Balachandran, N.K., 1968. Infrasound at long range from Saturn V, 1967, *Science,* **162**(3858), 1116–1120.

Evers, L.G. & Siegmund, P., 2009. Infrasonic signature of the 2009 major sudden stratospheric warming, *Geophys. Res. Lett.,* **36**(23), 1–6.

Evers, L.G., Van Geyt, A.R.J., Smets, P. & Fricke, J.T., 2012. Anomalous infrasound propagation in a hot stratosphere and the existence of extremely small shadow zones, *J. geophys. Res.,* **117**(D6), 1–10.

Hedlin, M.A.H., Drob, D., Walker, K. & de, Groot-Hedlin C., 2010. A study of acoustic propagation from a large bolide in the atmosphere with a dense seismic network, *J. geophys. Res.,* **115**(B11), 1–17.

Le Pichon, A., Vergoz, J., Blanc, E., Guilbert, J., Ceranna, L., Evers, L. & Brachet, N., 2009. Assessing the performance of the International Monitoring System's infrasound network: geographical coverage and temporal variabilities, *J. geophys. Res.,* **114**(D8), 1–15.

McIntyre, M.E. & Palmer, T.N., 1984. The 'surf zone' in the stratosphere, *J. Atmos. Terr. Phys.,* **46**(9), 825–849.

Melton, B. & Bailey, L., 1957. Multiple signal correlators, *Geophysics,* **22**(3), 565–588.

Nippress, A. & Green, D.N., 2017. Sensitivity of the International Monitoring System infrasound network to elevated sources: a western Eurasia case study, *Geophys. J. Int.,* **211**(2), 920–935.

Popova, O.P. *et al.*, 2013. Chelyabinsk airburst, damage assessment, meteorite recovery, and characterization, *Science,* **342**(6162), 1069–1073.

Smart, E. & Flinn, E.A., 1971. Fast frequency-wavenumber analysis and fisher signal detection in real-time infrasonic array data processing, *Geophys. J. R. astr. Soc.,* **26**(1–4), 279–284.

Smets, P.S.M., Evers, L.G., Näsholm, S.P. & Gibbons, S.J., 2015. Probabilistic infrasound propagation using realistic atmospheric perturbations, *Geophys. Res. Lett.,* **42**(15), 6510–6517.

Smets, P. S.M., Assink, J.D., Le Pichon, A. & Evers, L.G., 2016. ECMWF SSW forecast evaluation using infrasound, *J. geophys. Res.,* **121**(9), 1–14.

Wessel, P. & Smith, W.H.F., 1991. Free software helps map and display data, *EOS, Trans. Am. geophys. Un.,* **72**(41), 441.

SUPPORTING INFORMATION

Supplementary data are available at *GJI* online.

Figure S1.
Figure S2.
Figure S3.

Please note: Oxford University Press is not responsible for the content or functionality of any supporting materials supplied by the authors. Any queries (other than missing material) should be directed to the corresponding author for the paper.